

## Sol-Gel Transition of Concentrated Colloidal Suspensions

Sara Romer,<sup>1,2</sup> Frank Scheffold,<sup>1</sup> and Peter Schurtenberger<sup>1</sup>

<sup>1</sup>University of Fribourg, CH-1700 Fribourg, Switzerland

<sup>2</sup>Polymer Institute, ETH Zurich, CH-8092 Zurich, Switzerland

(Received 21 January 2000)

Diffusing-wave spectroscopy (DWS) was used to follow the sol-gel transition of concentrated colloidal suspensions. We present a new technique based on a sandwich of two scattering cells aimed to overcome the problem of nonergodicity in DWS of solidlike systems. Using this technique we obtain quantitative information about the microscopic dynamics all the way from an aggregating suspension to the final gel, thereby covering the whole sol-gel transition. At the gel point a dramatic change of the particle dynamics from diffusion to a subdiffusive arrested motion is observed. A critical-power-law behavior is found for the time evolution of the maximum mean square displacement  $\delta^2$  probed by a single particle in the gel.

PACS numbers: 82.70.Dd, 82.70.Gg

Aggregation and gelation of concentrated colloidal suspensions is a fascinating topic both from a fundamental as well as from a technological point of view. On one hand, colloidal gels are ideal models for the study of the internal dynamics and elasticity of highly disordered networks. On the other hand, sol-gel processes are widely used in the industry, in various materials preparations, as for instance the powder processing of ceramics [1]. A considerable amount of experimental and theoretical works as well as computer simulations has been carried out in the area of colloidal aggregation and cluster formation [2–4]. In a series of recent papers different groups have studied the properties of fractal colloidal gels at very low volume fractions which are accessible by static and dynamic light scattering [2]. However, little is known about the important case of high density colloidal gels where the local structural and dynamical properties differ substantially from diluted samples due to the high space filling of the particles. Previous studies in dense systems have addressed the macroscopic phase behavior of depletion gels [4] and the viscoelastic properties of nanoscopic size particle gels [5]. Structural information about the latter systems has been obtained by light and neutron scattering [6]. To understand however the viscoelastic properties of high density gels it is indispensable to have knowledge of the particle dynamics on length scales much smaller than the size of the individual particles, since the particle motion will be constrained to such small dimensions. Another most interesting subject is the time evolution of these local properties at the transition from sol to gel since it is this transition process that determines the final properties of the gel.

In this Letter we report on a study of the sol-gel transition of highly concentrated turbid colloidal suspensions using diffusing-wave spectroscopy (DWS) [7]. We induced the destabilization of a colloidal suspension using a novel catalytic technique leading to fully reproducible results over days and weeks. In addition we present an extension of DWS to the regime of nonergodic light scattering, thereby allowing the investigation of the microscopic par-

ticle dynamics from a stable suspension to the final stages of the gel in a single experiment.

The measurements were performed on a destabilized solution of polystyrene spheres, diameter  $d = (298 \pm 20)$  nm, at  $\Phi = 20\%$  volume fraction in a buoyancy-matching mixture of water and heavy water. One of the major problems in the study of concentrated colloidal gels is the appearance of spatial inhomogeneities in the destabilization process, in particular, if reproducibility is demanded throughout the whole sol-gel transition. To solve this problem we induced the coagulation of the electrostatically stabilized suspension with an *in situ* variation of the ionic strength without any local gradient using an enzyme-catalyzed internal chemical reaction (the urease catalyzed hydrolysis of urea [1]). In the stable suspension the urea represents 10% of the solvent volume. To destabilize the system we added urease at a temperature  $T \approx 3\text{--}5^\circ\text{C}$  where its activity is sufficiently reduced. The urease concentration (125 units for 1 ml of  $\text{H}_2\text{O}$  and  $\text{D}_2\text{O}$ , urease from Boehringer Mannheim GmbH) was chosen such that the aggregation and gelation at the selected temperatures ( $20^\circ\text{C}$ ,  $35^\circ\text{C}$ ) take place slowly over a period of hours or days to ensure complete gelation while the ionic strength of the solvent saturates and remains constant (but high) already after ca. 60–90 min (as determined by conductivity measurements at  $20^\circ\text{C}$ ). The gels appear homogeneous and their features are fully reproducible. We investigate the onset of aggregation and follow the sol-gel transition in this extremely turbid sample using DWS in transmission geometry. In the case of DWS light is scattered multiply in the sample and intensity fluctuations are due to the cumulative motion of all scattering particles along photon diffusion paths of length  $s$ . This allows one to study the particle dynamics in strongly turbid systems on very small length scales down to less than 1 nm [8]. For the particle size  $d/\lambda$  and volume fraction used in our experiments we can relate directly the correlation function of the scattered light intensity to the mean square displacement  $\langle \Delta r(\tau)^2 \rangle$  of the scatterers:

$g_2(\tau) - 1 = \left\{ \int_0^\infty P(s) \exp[-(s/l^*)k_0^2 \langle \Delta r^2(\tau) \rangle] ds \right\}^2$  [8]. The distribution of path lengths  $P(s)$  can be calculated within the diffusion model and depends only on the sample geometry (for details see Ref. [8]). Our DWS setup consists of a solid state laser ( $\lambda = 532$  nm) where the beam is expanded to a diameter of about 7 mm and illuminates the sample as a uniform planar source. The transport mean free path  $l^*$ , a measure for the sample turbidity, was obtained from a static transmission measurement relative to a sample of known  $l^*$  [9]. We find a value for  $l^*$  of  $13.7 \pm 1.4 \mu\text{m}$  which is in agreement with the value  $l^* = 15 \mu\text{m}$  expected for a suspension of hard spheres (in a solvent with 10% urea) [10]. For the short time diffusion coefficient in the stable suspension ( $T = 20^\circ\text{C}$ ) we find  $D(\Phi) = 0.75 \mu\text{m}^2/\text{s}$  which is smaller than the value expected for a dilute suspension ( $D_0 = 1.4 \mu\text{m}^2/\text{s}$ ) due to particle interactions [10]. During aggregation and gelation we monitor the static transmission which allows us to determine changes of  $l^*$  due to a modified microstructure [10]. An increase of about 30% in  $l^*$  is observed for the early stages of aggregation while later the value of  $l^*$  exhibits only minor changes and can be considered constant.

Figure 1(a) displays a sequence of typical intensity autocorrelation functions  $g_2(\tau) - 1$  during destabilization, where  $\tau$  is the correlation time. At early stages, clusters form due to particle aggregation and the decay of the correlation function shifts to higher correlation times due to the slower motion of the clusters. Gelation occurs when a single cluster fills the entire sample volume. After the sol-gel transition we observe that the correlation function  $g_2(\tau) - 1$  does not decay to zero but remains finite [inset, Fig. 1(a)]. We identify the gel point  $t_{\text{gel}}$  by the emergence of this nonergodic scattering signal. Qualitatively this is supported by our observation that this time coincides with a macroscopic liquid-solid transition. Before  $t_{\text{gel}}$  we observe that the sample shows still viscous flow upon tilting while afterwards it does not. In a standard light scattering experiment nonergodic contributions complicate the interpretation of the experimental data significantly [11]. In fact, in solidlike media, such as gels, scatterers are localized near fixed average positions and therefore are only able to execute limited thermally driven excursions, probing only a small fraction of all statistically possible spatial configurations of the system. As a consequence the measured time-averaged intensity correlation function is different from the ensemble-averaged correlation function. For dilute, nonergodic systems different methods have been described to properly average the experimental data [11]. For example, the sample can be rotated or translated while the correlation function is collected, leading to an additional decay proportional to the rotation/translation speed. In principle, this method can be directly transferred to turbid samples. However, for fragile systems with rapidly changing microstructure, the use of this method is problematic since it implies relatively high rotation/translation frequencies (10–100 Hz) in order to limit the data acquisition time.

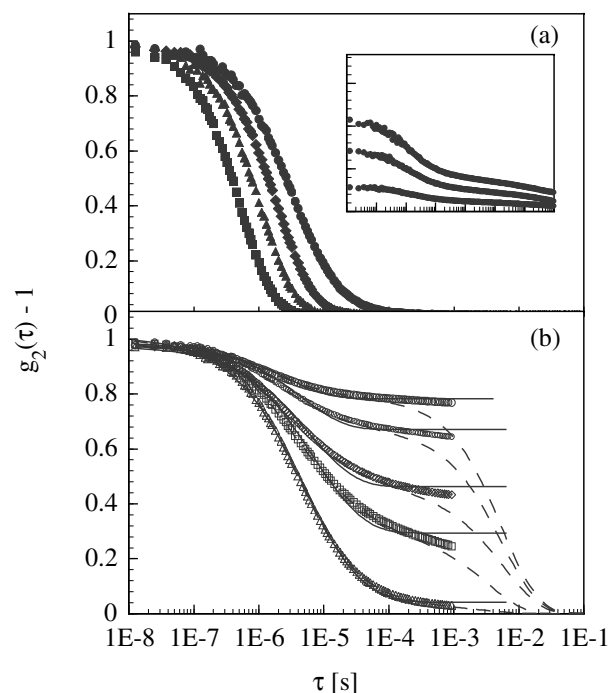


FIG. 1. Intensity autocorrelation function  $g_2(\tau) - 1$  during aggregation and gelation at  $T = 20^\circ\text{C}$ ; (a) stable 298 nm suspension (20% vol. fract.) at  $t = 0$  min and time evolution after destabilization for  $t = 11, 16,$  and  $82.5$  min. Inset: Repeated (time-averaged) measurements of  $g_2(\tau) - 1$  in the gel state (single layer) show the typical nonergodic light scattering signal of solidlike systems. (b) Ensemble-averaged correlation function  $g_2(\tau, L_1) - 1$  in the gel state after  $t = 108, 256, 734, 4683,$  and  $14400$  min determined from the two-cell setup using Eq. (1). The solid lines have been recalculated from the fit of Eq. (2) to the  $\langle \Delta r^2(\tau) \rangle$  data. The raw data  $g_2(\tau) - 1$  are also displayed (dashed lines).

To overcome the nonergodicity problem in the case of DWS we developed a noninvasive efficient new method which intrigues by its simplicity. We prepared a sandwich consisting of two independent glass cells (thickness  $L_2 = L_1 = 1$  mm) where the first cell contains the sample to be investigated, which can be either a stable ergodic or a gelling nonergodic sample. The second cell, which serves to properly average the signal of the first cell only, contains an ergodic system with very slow internal dynamics and moderate turbidity. A static speckle spot of characteristic size  $\lambda^2$  at the cell interface is diffusively broadened by the presence of the second layer to a size  $L_2^2 \gg \lambda^2$ . Since the second layer is ergodic we obtain a two-dimensional average over all speckle spots within the same area  $L_2^2$ . This scheme is therefore much more efficient than translating or rotating the sample which always implies one-dimensional motion. The correlation function  $g_2(\tau) - 1$  of the two-cell setup can be expressed by the joint distribution function  $P(s_1, s_2)$  of path segments  $s_1, s_2$  in both layers:  $g_2(\tau) - 1 = \left\{ \int_0^\infty P(s_1, s_2) \exp[-(s_1/l_1^*) \times k_1^2 \langle \Delta r_1^2(\tau) \rangle] \exp[-(s_2/l_2^*) k_2^2 \langle \Delta r_2^2(\tau) \rangle] ds_1 ds_2 \right\}^2$ . In the case of independent scattering in both layers (i.e., no loops of the scattering paths between the two layers)

this distribution factorizes  $P(s_1, s_2) \approx P(s_1)P(s_2)$  and therefore we can write the correlation function as a product of the correlation functions of the two independent cells:  $g_2(\tau) - 1 = [g_2(\tau, L_1) - 1][g_2(\tau, L_2) - 1]$  which we call the “multiplication rule.” The factorization of  $P(s_1, s_2)$  holds well if, e.g., the first layer has a high optical density  $L_1/l_1^* \gg 1$  while the second layer shows only moderate multiple scattering  $L_2/l_2^* \gtrsim 1$ . From this it is possible to determine directly the contribution of the first cell by dividing the signal of the two-cell sandwich  $g_2(\tau) - 1$  with the separately measured autocorrelation function  $g_2(\tau, L_2) - 1$  of the ergodic system in the second cell:

$$g_2(\tau, L_1) - 1 = [g_2(\tau) - 1]/[g_2(\tau, L_2) - 1]. \quad (1)$$

A general theoretical treatment of DWS in multilayered media has been developed by Skipetrov and Maynard [12]. Numerical application of their results (with the properties discussed above) reveals that the relative deviation from Eq. (1) is less than  $10^{-3}$  for  $\tau = (1/5)\tau_2$ , rapidly decaying to zero for a shorter correlation time. Here  $\tau_2$  denotes the decay time of  $g_2(\tau, L_2) - 1$  [13].

We adjusted the scattering properties of the second sample cell using a 1.5% dispersion of polystyrene spheres, diameter 810 nm, in a mixture of water and glycerol (with a solvent volume ratio of 40:60). From Mie theory we calculated a value for the total thickness of the sample  $L_2 \approx 2l^*$ . Together with the high viscosity of the solvent this leads to a relatively slow almost exponential decay  $g_2(\tau, L_2) - 1 \approx \exp[-t/\tau_2]$  (decay time  $\tau_2 \approx 6$  ms). Initially this decay is separated by about 4 orders of magnitude from the decay of the stable suspension and therefore allows the coverage of a broad range of correlation times during the destabilization and gelation process. The light, passing through both cells, is measured in transmission geometry with a single mode fiber and subsequently analyzed with a digital correlator. With this setup we are able to determine experimentally the correlation function of the first (gelling) sample  $g_2(\tau, L_1) - 1$  over a wide interval of correlation times from 10 ns to 1 ms covering the whole sol-gel transition without any modification or mechanical disturbance of the setup.

As long as the dynamics of the first sample are ergodic, and therefore fast, we do not see the contribution of the second cell which decays on a long time scale where the correlation function of the first sample has already decayed to zero. As shown in Fig. 1(b) this situation changes however during destabilization. After the gel point the system becomes solidlike and the correlation function of the gelling sample does not decay to zero but exhibits almost a plateau with a remaining decay on very long time scales far out of the time window covered by our experiments. At this point we can also see the additional “forced” decay of the second cell [Fig. 1(b)]. With increasing time the gel becomes more and more dense which is manifested by an increase in the plateau height. Furthermore the plateau-like shape of the correlation function now becomes more clear

since the internal restructuring is slowed down. These results demonstrate that the new two-cell technique can be easily applied in practice and offers the advantage of high statistical accuracy.

For a quantitative investigation of the microscopic particle dynamics we analyzed the particle mean square displacement  $\langle \Delta r^2(\tau) \rangle$  as calculated from  $g_2(\tau, L_1) - 1$  and  $l^*$  [8]. Figure 2 displays the evolution of  $\langle \Delta r^2(\tau) \rangle$  during the destabilization process. Initially we observe diffusion of the particles over the whole accessible time range which is manifested by the linear dependence of  $\langle \Delta r^2(\tau) \rangle$  on  $\tau$  [Fig. 2(a)]. In the first stage the formation of large aggregates and clusters leads to a dramatic slowdown of the single particle diffusion. Later the long time behavior of  $\langle \Delta r^2(\tau) \rangle$  becomes more and more constrained. In this regime, before gelation, the particle shows simple diffusive motion only a length scale of  $\sqrt{\langle \Delta r^2 \rangle} \approx 1-2$  nm, representing only a small fraction of the particle diameter [Fig. 2(a)]. At the gel time the short time behavior changes qualitatively from diffusion to a subdiffusive motion well described by a power law  $\langle \Delta r^2(\tau) \rangle \propto \tau^p$ . We find, within

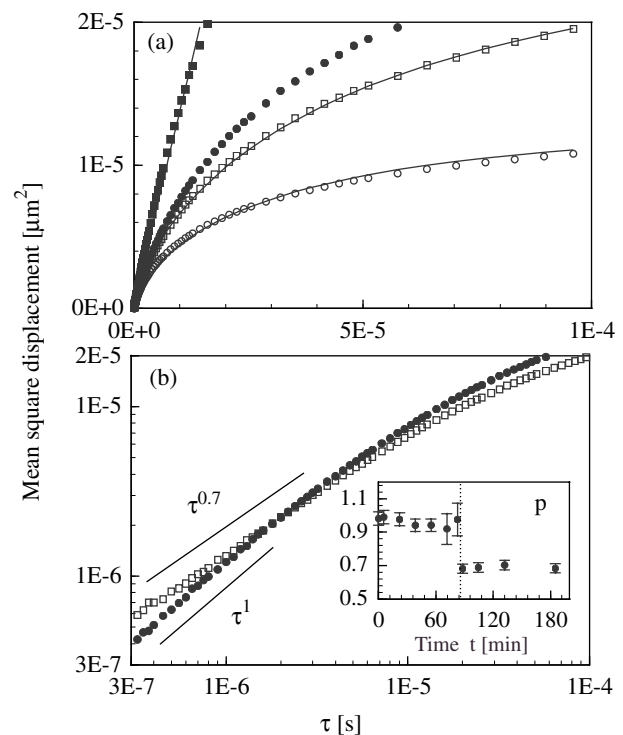


FIG. 2. (a) Mean square displacement  $\langle \Delta r^2(\tau) \rangle$  at different stages  $t = 0, 82.5, 88,$  and  $132$  min of the gelation process (full symbols before the gel point and open symbols after the gel point). Within the measured range of correlation times  $\langle \Delta r^2(\tau) \rangle$  changes from a single diffusive behavior (full squares) to a slowed down constrained diffusion (full circles). The behavior in the gel state (open symbols) is well described by a subdiffusive motion [Eq. (2), solid lines]; (b) short time behavior of the mean square displacement close to the gel point (full circles:  $t = 82.5$  min, open squares:  $t = 88$  min):  $\langle \Delta r^2(\tau) \rangle \propto \tau^p$ . A qualitative change of the particle dynamics is observed at the gel point (inset, dashed line) changing from free diffusion ( $p = 1$ ) to a subdiffusive motion ( $p = 0.7 \pm 0.05$ ).

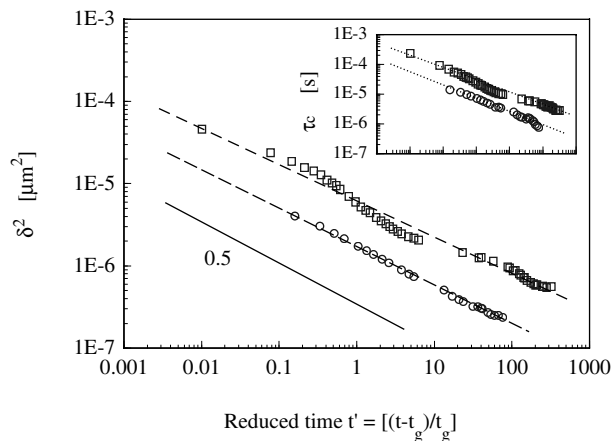


FIG. 3. Critical time evolution of the maximum mean square displacement  $\delta^2$  and the characteristic decay time  $\tau_c$  (inset) after the gel point. The dashed lines are power-law fits to the  $\delta^2[t']$  data with exponents  $0.44 \pm 0.03$  (20 °C, open squares) and  $0.48 \pm 0.03$  (35 °C, open circles), where the error also takes into account the uncertainty in  $t_g$ . For  $\tau_c[t']$  the fit yields an exponent of  $0.4 \pm 0.03$  at 20 °C ( $0.45 \pm 0.03$  at 35 °C).

our time resolution, that the exponent for diffusion  $p = 1$  drops at the gel point and takes a value of  $p \approx 0.7$  for all  $t > t_{\text{gel}}$  [Fig. 2(b)]. This indicates that already close to the gel point  $t_{\text{gel}}$  almost all particles are connected to the gel network. Once the gel spans over the whole sample the signal is dominated by a broad distribution of elastic gel modes. We find that in the gel state the average mean square displacement is well described for all  $\tau$  by a stretched exponential,

$$\langle \Delta r^2(\tau) \rangle = \delta^2 [1 - e^{-(\tau/\tau_c)^p}], \quad (2)$$

leading to a plateau at long times (with  $p = 0.7 \pm 0.05$ ) [Fig. 2(a)].

This behavior is qualitatively similar to what is found in dilute fractal gels, however, with reduced values for  $\tau_c$ ,  $\delta^2$  reflecting the compactness of the dense gel [2]. These results suggest that the exponent  $p = 0.7 \pm 0.05$  is a common feature of colloidal gels even when the development of a loose fractal structure is suppressed due to the high space filling.

The plateau height  $\delta^2$  and the characteristic decay time  $\tau_c$  are important quantities related to the gel microstructure.  $\delta^2$  is a measure for the distance an individual particle can move away from its average position while  $\tau_c$  characterizes the spectrum of excited modes in the gel. Both values therefore characterize the compactness and rigidity of the gel. We analyzed the time evolution of  $\delta^2$  and  $\tau_c$  for two different temperatures  $T = 20$  °C and  $T = 35$  °C as a function of the reduced time  $t' = (t - t_g)/t_g$ . We find that while the gel gets more compact its elastic modes shift to higher frequencies, i.e., shorter time scales. A distinct power-law decrease is observed as a function of  $t'$  with the same exponent of the order of 0.4–0.5 for both  $\delta^2[t']$  and  $\tau_c[t']$  (Fig. 3), therefore the ratio  $\delta^2[t']/\tau_c[t'] \approx 0.25 \pm 0.05$   $\mu\text{m}^2/\text{s}$  is found to be almost constant over the whole

gelation process. We find this value in surprisingly good agreement with a simple model for the particle motion in a colloidal gel recently developed by Krall and Weitz [2]. For gels with a fractal dimension  $d_f = 1.9$  (diffusion limited aggregation) they find  $\delta^2[t']/\tau_c[t'] \approx 1.2D_0\Phi^{0.9} = 0.39$   $\mu\text{m}^2/\text{s}$ ; here  $D_0 = 1.4$   $\mu\text{m}^2/\text{s}$  denotes the free particle diffusion constant ( $T = 20$  °C) [14]. Further studies are now underway to investigate this dependence on concentration as well as on temperature and interaction potential (ionic strength) in order to obtain a comprehensive understanding of all properties affecting the microscopic dynamics of these fascinating materials.

We are grateful to Ludwig Gauckler for introducing us to the enzyme-catalyzed internal chemical reaction technique. We thank Sergey Skipetrov, Markus Hütter, and Thomas Gisler for useful comments and discussions. We kindly acknowledge Frank Horn, University of Freiburg (Germany), who provided us with the 298 nm polystyrene particles. We gratefully acknowledge financial support from the Swiss National Science Foundation.

- [1] L.J. Gauckler, T. Graule, F. Baader, *Mater. Chem. Phys.* **2509**, 1–25 (1999), and references therein.
- [2] A.H. Krall and D.A. Weitz, *Phys. Rev. Lett.* **80**, 778 (1998); M. Carpineti and M. Giglio, *Phys. Rev. Lett.* **68**, 3327 (1992).
- [3] E. Dickinson, *J. Colloid Interface Sci.* **225**, 2–15 (2000); special issue on *J. Sol-Gel Sci. Technol.*, edited by A. Hasmy and R. Julien [*J. Sol-Gel Sci. Technol.* **15**, 129 (1999)].
- [4] W.C.K. Poon *et al.*, *Faraday Discuss.* **112**, 143–154 (1999).
- [5] W.-H. Shih *et al.*, *Phys. Rev. A* **42**, 4772 (1990), and references therein.
- [6] C.D. Muzny, G.C. Straty, and H.J.M. Hanley, *Phys. Rev. E* **50**, R675 (1994).
- [7] G. Maret and P.E. Wolf, *Z. Phys. B* **65**, 409 (1987); D.J. Pine, D.A. Weitz, P.M. Chaikin, and E. Herbolzheimer, *Phys. Rev. Lett.* **60**, 1134 (1988).
- [8] D.A. Weitz and D.J. Pine, in *Dynamic Light Scattering*, edited by W. Brown (Clarendon Press, Oxford, 1993).
- [9] P.D. Kaplan, M.H. Kao, A.G. Yodh, and D.J. Pine, *Appl. Opt.* **32**, 21 (1993); **32**, 3828 (1993).
- [10] S. Fraden and G. Maret, *Phys. Rev. Lett.* **65**, 512 (1990); X. Qiu, X.L. Wu, J.Z. Xue, D.J. Pine, D.A. Weitz, and P.M. Chaikin, *Phys. Rev. Lett.* **65**, 516 (1990).
- [11] J.Z. Xue, D.J. Pine, S.T. Milner, X.L. Wu, and P.M. Chaikin, *Phys. Rev. A* **46**, 6550 (1992); P.N. Pusey and W. van Meegen, *Physica (Amsterdam)* **157A**, 705 (1989).
- [12] S.E. Skipetrov and R. Maynard, *Phys. Lett. A* **217**, 181–185 (1996); F. Scheffold, S.E. Skipetrov, S. Romer, and P. Schurtenberger (to be published).
- [13] A patent application for this method was filed with the Suisse Institute of Intellectual Property on 27 February 2000 under No. 200 0335/00.
- [14] We estimated the average cluster size from the simple model that gelation occurs when the whole sample volume is filled up uniformly:  $2R_c \approx d\Phi^{-1/(3-d_f)}$  [2,3].